Journal of Nuclear Materials 377 (2008) 444–448

Contents lists available at ScienceDirect

Journal of Nuclear Materials

journal homepage: www.elsevier.com/locate/jnucmat

Behavior of metallic precipitate in an irradiated simulated fuel

Y.H. Jung *, K.H. Kang, I.H. Jung, J.M. Park, G.S. Kim, Y.S. Choo, K.C. Song, K.P. Hong

Korea Atomic Energy Research Institute,150, Dukjin-Dong, Yuseong-gu, Daejeon, 305-353, Republic of Korea

ARTICLE INFO

Article history:
Received 31 October 2006
Accepted 8 March 2008

PACS:
25.85.Ge

ABSTRACT

A simulated fuel specimen which was irradiated at the HANARO research reactor up to 3300 MWd/tU of a burn-up at the condition of 36 kW/m of a maximum linear power was studied by a shielded EPMA (Electron Probe Micro-Analyzer). In order to obtain an accurate analysis results, chemical and EPMA analyses were also performed on un-irradiated fresh simulated fuel, the results of which were compared with those of the irradiated simulated fuel. This study concentrated on the metallic precipitates of the irradiated simulated fuel specimen which contained lots of fission products. Among the several properties of the metallic precipitate, its size and composition were investigated. A large metallic inclusion was also observed in the irradiated simulated fuel, from which X-ray photographs were taken to analyze its properties.

1. Introduction

At present, various kinds of fuels are used in different reactor types. To investigate the thermal and mechanical properties of these fuels it is very important to perform a fuel performance analysis. A simulated fuel is widely used to examine the properties of an active nuclear fuel by adding surrogates to a uranium fuel. Furthermore, the irradiation behavior of a simulated fuel is quite similar to that of an irradiated fuel with regards to the behaviors of several dominant fission products [1].

Previous studies by adopting a post-irradiation test have been performed for an irradiated DUPIC (Direct Use of Spent PWR Fuel in CANDU Reactors) fuel, which was fabricated from spent fuel with an oxidation and a reduction process [2-4]. Because a fission product affects the electric and thermal conductivities of a fuel, a large quantity of it changes the fuel performance of a fuel especially for high burn-up fuels, therefore, characterizing a metallic precipitate through a post irradiation examination is important. Molybdenum is the least noble element in such alloys and it is known that this type of precipitate has a hexagonal structure and its homogeneity is usually maintained. It is also widely known that the density of this precipitate in a fuel at a high temperature increases at around a fractional fuel radius = $0.6(r/r_0)$, which results from a movement of Mo and Ru to a lower temperature region due to an oxidation [5]. The oxygen potential of a dioxide, MoO_2, in an equilibrium state with in alloys, is comparable to the oxygen potential of a fuel within its homogeneity region [6].

The property changes in a highly irradiated nuclear fuel, such as, either an irradiated simulated fuel with various fission products or a high burn-up long cycle fuel, affect the characteristics of its fuel–thermal conductivity, fission gas release, creep etc. In particular, the thermal conductivity of a metallic precipitate is 10 times higher than other fission products. The main purpose of this study is to investigate the behavior of a metallic precipitate in a fuel and its effect on fuel's properties. During performing analysis, a large metallic inclusion was found in the irradiated simulated fuel. In this paper some discussions are also provided in this regard.

2. Experimental preparations

EPMA (Electron Probe Micro Analyzer, SX-50R, CAMECA, FRANCE), SEM (Philips XL-30) were used to identify the major constituents of the metallic precipitates in this study. The specimen holder as a part of the equipment was shielded from a radiation leakage and WDS (wavelength dispersive spectroscopy) count windows containing lead and tungsten were used to permit an analysis of the irradiated nuclear fuel. In this EPMA, the allowed radiation activity was up to 3.7×10^{10} Bq.

Molybdenum, ruthenium, rhodium and palladium were used at an electron acceleration potential of 15 kV and a beam current of 20 nA. Molybdenum was analyzed by using the $L\alpha_1$ X-ray line and a PET (Pentaerythritol Tetrakis) diffracting crystal in WDS-1. The others were analyzed by using the $L\alpha_1$ X-ray line and a PET diffracting crystal in WDS-2.

It has been suggested that an electron beam has to be focused exactly at the center of a precipitate and perpendicular to it, to characterize small metallic precipitates. At the same time, even a tiny vibration should be excluded during a measurement. For this, the stage motor was turned off during a measurement and the electron beam was irradiated at a fixed mode with a 1 μm beam size.

* Corresponding author. Tel.: +82 42 868 8459; fax: +82 42 868 8420.
E-mail address: nyhjung@kaeri.re.kr (Y.H. Jung).

0022-3115/$ - see front matter © 2008 Elsevier B.V. All rights reserved.
doi:10.1016/j.jnucmat.2008.03.023

The procedure established in this investigation has been applied to an irradiated simulated fuel. In such a way the γ-activity was maintained within the tolerances specified above. Although a specimen's size has to be maintained small enough, its volume could be managed with a manipulator in a hot cell. After cutting the specimen into a manageable size with the manipulator, the specimen was hot mounted with a conducting resin at 150 °C and 0.6 MPa. Too thin a specimen is apt to be broken during a hot mounting, so its depth was cut to about 5 mm at first. And finally, a specimen of $2.5 \times 5 \times 1.5$ mm^3 was fabricated by repeating the mounting and cutting processes several times to decrease the radiation level by using a manipulator. The specimen was subsequently polished in a conventional manner with a γ-monitoring, until the activity was considered to be low enough for handling it.

To enhance the electric conductivity, silver paint (Leistsilver 2000 silver paint, TED PELLA, INC.) was spread over the surface of the specimen. Precautions were also taken to avoid any contamination of the SX-50R instrument. The mounted sample was cleaned with alcohol and held under a vacuum for ten hours to ensure that no loose particles remained.

2.1. Preparation of the fresh simulated fuel

A simulated fuel was fabricated by adding 14 representative chemicals, which corresponds to 35 000 MWd/tU of a burn-up in a PWR. To fabricate the simulated fuel, about 400 g of a mixed powder of 3.2 wt% slightly enriched uranium and natural uranium was milled in a dry attritor at 150 rpm for 15 min., which was replicated 5 times. Particle size of the raw powder was 3.28 μm, which was decreased to 1.68 μm after 1 turn and revealed 0.5 μm after 5 turns. Particle size was decreased ever more after continually repeating the steps. To reduce the friction between the surface of the pelletizing die and the pellet, Zn stearate solved in benzene was spread over to the surface of the die. Pelletizing was carried out at a pressure of about 1.65 ton/cm^2, and sintered at 1800 °C under a reduction condition (H_2 100%) for 10 h. No micro-cracking of the pellets was observed by a scanning electron microscopy.

2.2. Preparation of the irradiated simulated fuel

A specimen of an irradiated simulated fuel was irradiated at the HANARO research reactor at up to 3300 MWd/tU of a burn-up with 36 kW/m of a maximum linear power and 32 kW/m of an average linear power. The post irradiation examination was performed in the IMEF (Irradiated Materials Examination Facility) hot cell in KAERI.

Irradiation rig to retain the irradiated simulated fuel was fabricated with Al-6061 and its dimensions were 960 mm in length, 56 mm in diameter and 3.0 kg in weight. Cladding tube was fabricated with Zircaloy-4 with the dimensions of 0.66 mm in thickness, 10.08 mm in an inner diameter and 199 mm in length. Dimensions of the sintered pellet were 10 mm in length and 10.6 mm in diameter with a theoretical density of 10.07.

After an irradiation in HANARO, the specimen to observe the microstructure was taken at a 5 mm thickness with a diamond wheel at a position of 100 mm from the top of the cladding tube.

3. Results and discussion

3.1. Metallic precipitates of the fresh simulated fuel

To compare the concentration of the metallic precipitates results by the EPMA, a wet chemical analysis was carried out [7]. Table 1 shows these results. Column (a) in Table 1 presents the result of the wet chemical analysis. They agreed well with the initial concentration of the added chemicals as well as the results by the EPMA of column (b) in Table 1. The EPMA measurement was carried out by scanning a small area at a TV mode at a magnification of 20 000. In the case of a fixed mode, an error could occur from eliminating the precipitates extracted at the grain boundaries or the vacancies, so a large area was scanned. After setting up the characterizing conditions such as applying a voltage and current, a characterizing by the EPMA was accomplished for the metallic precipitates of the irradiated simulated fuel.

Table 1
Comparison of the concentrations between wet chemical and EPMA analysis (wt%)

Chemicals	Initial concentration of the added chemicals	Chemical analysis (a)	EPMA analysis (b)
Mo	0.43	0.45	0.39
Ru	0.22	0.24	0.27
Pd	0.09	0.03	0.19
Rh	0.05	0.07	0.05
Nd	0.44	0.46	0.48

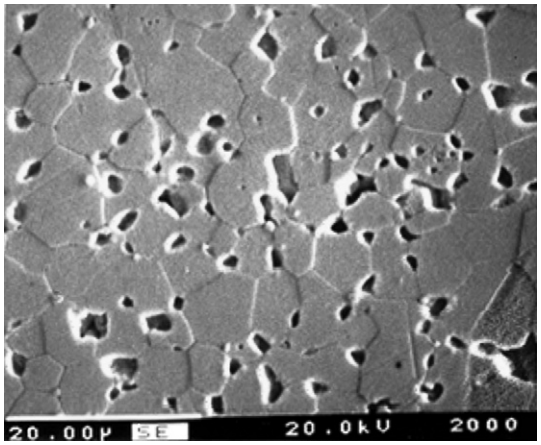

Fig. 1. Metallic precipitates image for the fresh simulated fuel ×2000.

Fig. 1 shows the spherical inter-granular metallic precipitates (0.5–1.0 μm diameter), uniformly distributed in the fresh simulated fuel matrix. They were extracted as metal or oxide precipitates during a sintering of the added chemicals in the UO_2 powder. It is understood that as the total composition is about 47.52 wt% in Table 1 and the U matrix element is analyzed as 51 wt%, it means that the induced electron beam was not correctly targeted at the spherical metallic precipitates and instead it was scattered over the shape of the surface. By representing them as an atomic percent by excluding uranium, Molybdenum 57.58 at.%, Ruthenium 35.40 at.% and Palladium + Rhodium 7.03 at.%. According to the micro structural features in the simulated fuel, it has a $\sigma + \varepsilon$ phase according to the metallic precipitate section of the Molybdenum–Ruthenium–Palladium phase diagram at 1700 °C [8,9].

3.2. Metallic precipitates of the irradiated simulated fuel

Fig. 2 shows a secondary electron image of the surface of the irradiated simulated fuel in the radial direction. From Fig. 2, it is observed that the grain size of the center part (a) is larger than that of the outer part (c). The centerline temperature of the irradiated simulated fuel was estimated to be about 2000 K by using the FEMAXI fuel performance code which accommodates the thermal conductivity level of a simulated fuel. Also the grain size of the center pellet was observed to be about 10–15 μm, which is increased

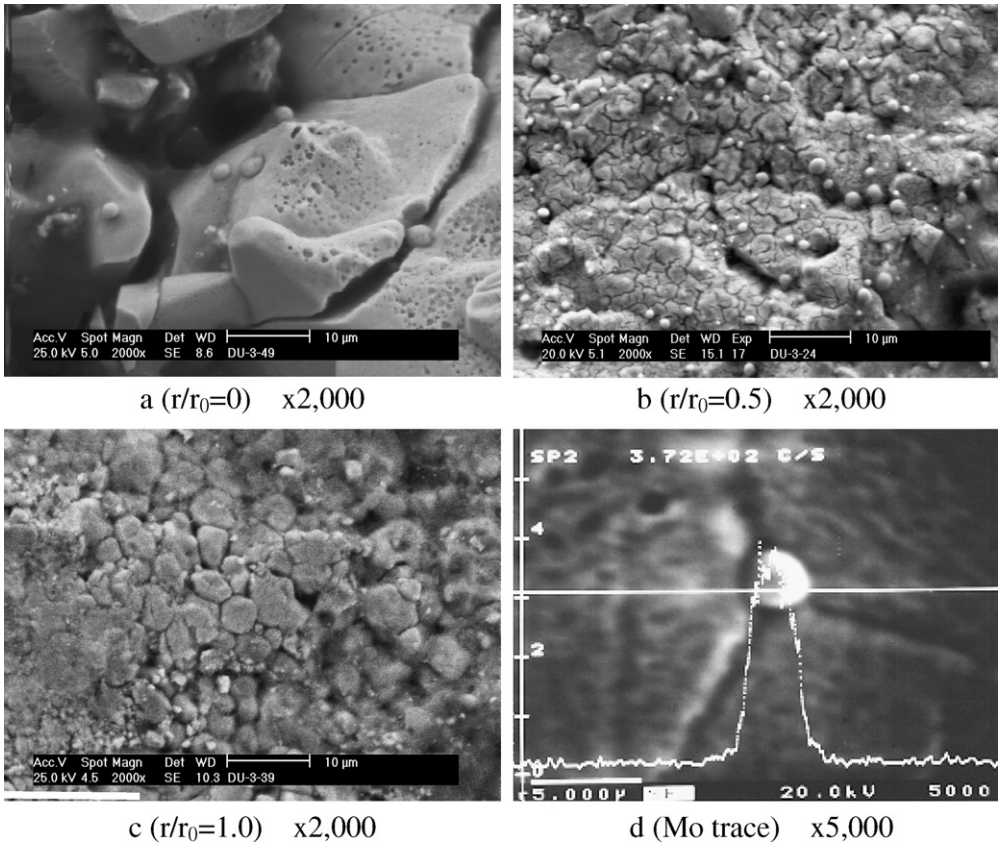

Fig. 2. Secondary electron image of the irradiated simulated fuel and Mo trace on the metallic precipitate: (a) $r/r_0 = 0$, (b) $r/r_0 = 0.5$, (c) $r/r_0 = 1$, and (d) Mo trace on the metallic precipitate $r/r_0 = 0.2$.

by about 1.5–1.7 times when compared with the initial state. When considering the grain size in relation to the irradiation condition, both the burn-up and temperature have an effect on the grain growth and particularly the centerline temperature has a greater effect on the grain growth because the burn-up is low in this case. Fig. 2(d) depicts a Mo trace for the metallic precipitate at $r/r_0 = 0.2$. The metallic precipitate is located on the grain boundary and has a spherical shape but it was also observed as both a precipitate in the grain or a spherical shape as shown in Fig. 2(a) and (c). Metallic precipitates were observed at the grain boundaries as well as the intra grains.

3.3. Discussion on the metallic precipitates

Fig. 3 depicts the distribution of the metallic precipitate in the radial direction. From the center of the specimen, 10 parts with the same distance of 400 μm were selected arbitrarily and ×200 SEM photos were taken. Among the several metallic precipitates, the average size was obtained from five different images. The metallic precipitates observed in the fresh simulated fuel were 0.5–1.0 μm, while those of the irradiated simulated fuel were 2–3.5 μm in diameter. It is believed that the initially produced precipitates during the sintering process were grown by a coalescence with the newly produced fission products during an irradiation. Also it was found that the size of the metallic precipitate became smaller from the center to the surface of a specimen.

Fig. 3(b) shows the quantitative results for the Mo element at 50 points in the radial direction. It is well known that Mo also exists as an oxide form in a fuel matrix. Because a metallic precipitate is distributed abnormally in a fuel, the analysis of Mo was performed with EPMA at the grain boundary rather than in the grain. Among the several EPMA methods, the TV mode was chosen with a magnification of 10000 times. Although the concentration of Mo may increase in a metallic precipitate, the trend of Mo can be estimated if an analysis is performed at an arbitrary point with the same distance in the radial direction. In Fig. 3(b), the concentration profile of the molybdenum dissolved in the fuel matrix, trend represents that the concentration of molybdenum at the fuel surface is scattered more so than that at it is center. The oxidized molybdenum was assumed to be dissolved in the oxide fuel matrix. This is a result of a fission process because oxygen cannot be completely bonded by the generated fission products [10]. Hence, the ratio of the molybdenum concentration in the alloys to the MoO_2 concentration in the fuel matrix is an indicator of a local oxygen potential of a fuel which is based on an equilibrium state [10]

$$[Mo]_{alloy} + [O_2]_{fuel} = [MoO_2]_{fuel} \quad (1)$$

Compositions of the precipitates observed at the grain boundaries and those of the intra grains were not different from each other. Namely, the concentrations of molybdenum and ruthenium tended to decrease as the r/r_0 increased. The reason for this phenomenon is assumed to be the higher oxygen concentration at the periphery. Molybdenum and ruthenium elements are likely to be in the form of the oxides when the concentration of oxygen is high. Because neutrons are generally absorbed in a fuel's surface region, which results in a higher fission rate there. Therefore, a higher oxygen concentration is maintained in a fuel's surface region due to the liberated oxygen from UO_2 during the nuclear fission reactions. The reason for a low concentration of molybdenum in the metallic precipitate in the fuel's surface region is that molybdenum is likely to be an oxide of MoO_2 at a higher oxygen concentration. The oxidized molybdenum of a fission product is assumed to dissolve in a fuel matrix with an abundant amount of oxygen [10].

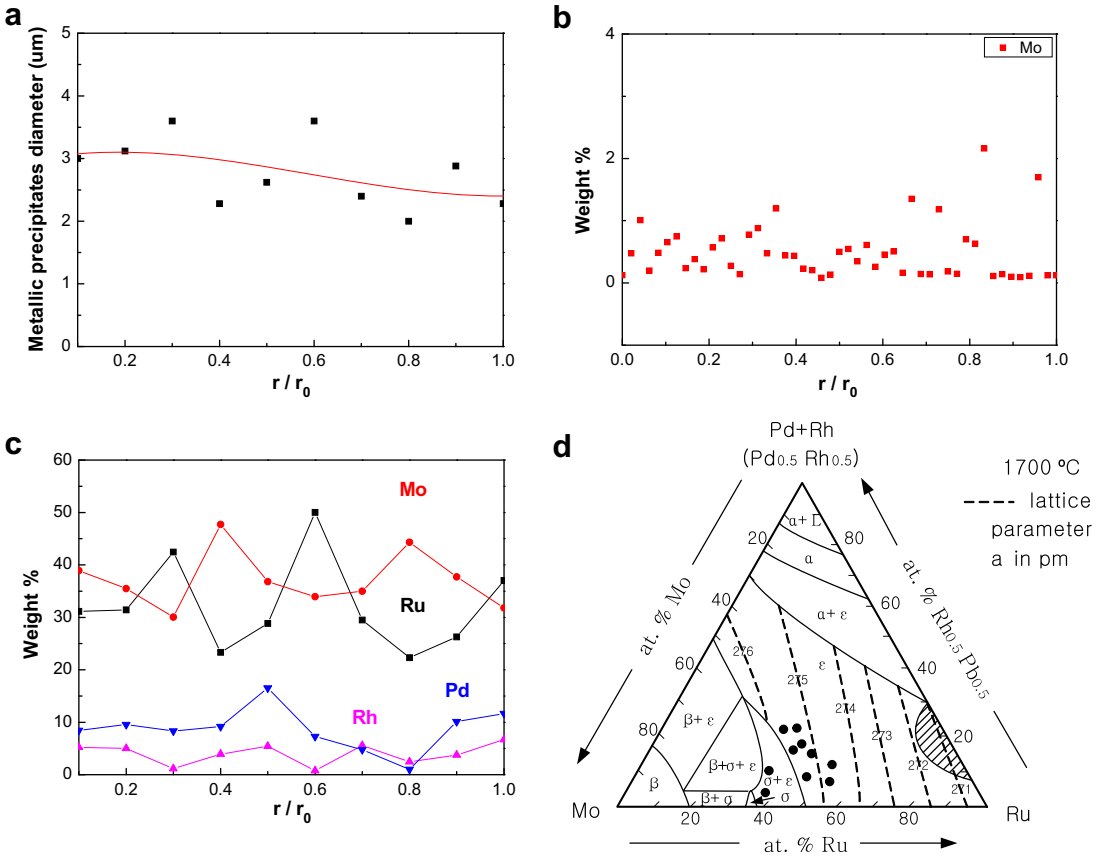

Fig. 3. Size, composition of the irradiated simulated fuels: (a) size of the metallic precipitate, (b) distribution of the Mo concentration (×10000), (c) weight percent of various metallic precipitates, (d) the hexagonal Mo–Ru–(Rh + Pd) precipitates of the irradiated simulated fuel. The compositions are projected onto the Mo–Ru–Rh0.5 Pd0.5 section at 1700 °C.

It was found that the concentration of Ru had a similar behavior of Mo with the same EPMA analysis methods. The data was also extracted by following the same procedure for Mo in Fig. 3(b). When considering a low burn-up of the irradiated simulated fuel, it is understood that the precipitates of the perovskite phases are developed during the fabrication process of the irradiated simulated fuel (oxide/reduction, slitting process). A ceramic nucleation cluster may develop during a sintering process and a solid solution diffusion process. Therefore, it is understood that the main reason for a size change of the metallic precipitate at different regions is its various formations at different temporal conditions during an irradiation in the HANARO.

Fig. 3(d) depicts a projection of the radial concentration change for the metallic precipitate section of the Molybdenum–Ruthenium–Palladium phase diagram at 1700 °C [11]. At the regions of $r/r_0 = 0.4$ and $r/r_0 = 0.8$, the phase of the lattice parameter was identified as $\sigma + \varepsilon$ phases and the others were ε phases.

3.4. Discussion on a large metallic inclusion

Generally the size of a metallic precipitate is 1–2 μm. A large metallic inclusion was observed during the investigation of the irradiated simulated pellet. Fig. 4 shows a photograph of a typical large precipitate observed in the specimen at $r/r_0 = 0.3$, where this precipitate has higher concentrations of palladium and ruthenium than the usual metallic precipitates, and it is accompanied by a barium oxide phase in the adjacent region. There happens to be a grain wetting when the precipitates are melted during an irradiation but this was not found in Fig. 4. Also it is not evident that a laminar structure was formed when several metals were melted during the irradiation process. Fig. 5 shows the SEM photographs for the circled region of Fig. 4 and the characteristic X-ray photographs. In the bulk, a metallic inclusion shows a higher concentration of palladium and molybdenum than the usual precipitates. From Fig. 5, it is observed that a large metallic inclusion did not form a spherical shape. This abnormal shape might be due to a temperature distribution in the pellet during an irradiation. Fig. 6 shows the weight percent for the quantitative line in Fig. 5. In the outer region of the inclusion, Pd and Ni are dominant, while in the center region, Mo and Ru are dominant. It is also noted that Fe, Ni, Cr were found in small amounts, which were initially intro-

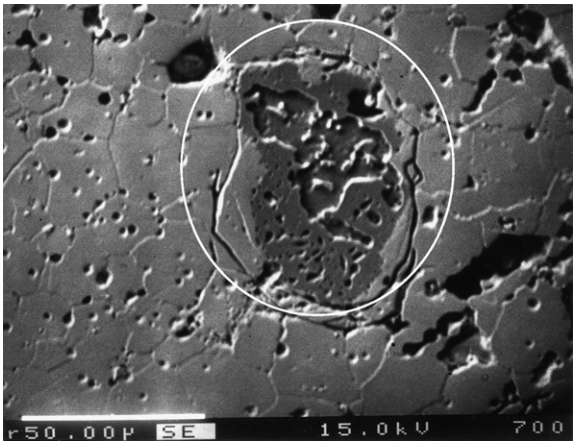

Fig. 4. SEM microscopy of the irradiated simulated fuel ×700.

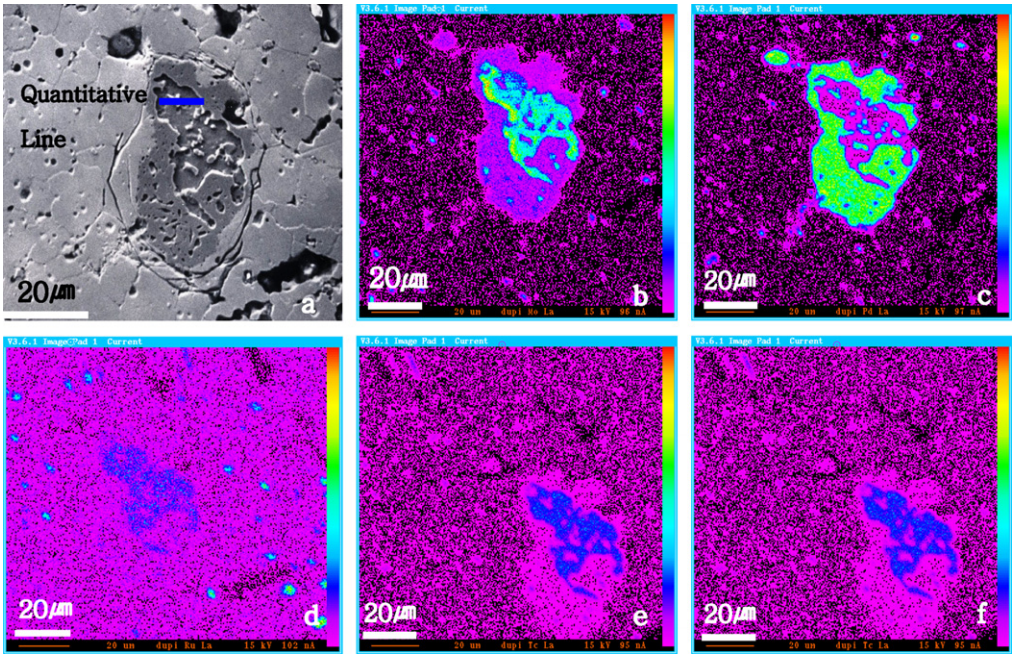

Fig. 5. Secondary image photomicrograph and characteristic X-ray photographs ($r/r_0 = 0.3$): (a) microstructure, (b) Mo Lα, (c) Pd Lα, (d) Ru Lα, (e) Tc Lα, and (f) Rh Lα.

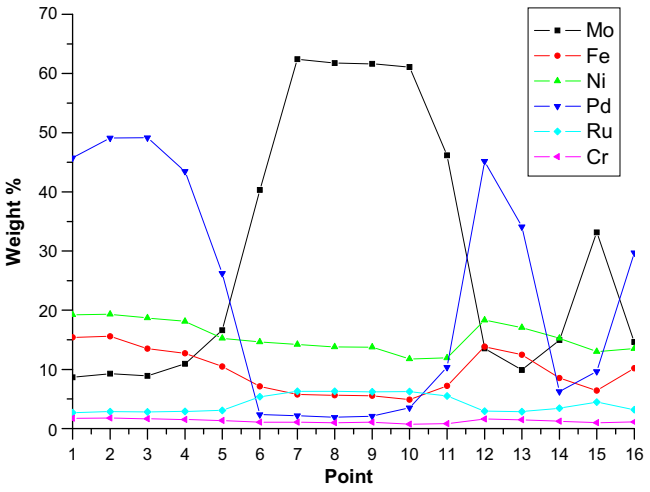

Fig. 6. Weight percentage of various elements in Fig 5(a) (quantitative line).

duced during the milling process of the simulated fuel. It is also understood that even though the content of the impurity is small, it would be significant because the metallic precipitates would accumulate around the impurities during irradiation. However, more investigations should be undertaken not only by a detailed post-irradiation test but also by using various kinds of specimen fuels.

4. Conclusion

A detailed analysis was performed for the metallic precipitates of an irradiated simulated fuel and the results were compared with those of a fresh simulated fuel. From the results, it was suggested that the metallic precipitate was formed during the fabrication process of the simulated fuel because the irradiation period was not long enough in the HANARO test reactor. The oxidation and reduction processes had an effect on the formation of the metallic precipitates. Also a large metallic inclusion was found and some quantitative results were provided including the weight percentage for some major elements. To establish more reliable results for a metallic precipitate and a large metallic inclusion in an irradiated simulated fuel, more post-irradiation tests should be performed with various kinds of fuels. It is believed that the approach of this study will be helpful in analyzing the performance of impurities in an irradiated fuel.

References

[1] P.G. Luctuta, R.A. Verral, Hj. Matzke, B.J. Palmer, J. Nucl. Mater. 178 (1991) 48.
[2] M.S. Yang, B.B. Kim, S.S. Kim, I.H. Jung, in: Proceedings of the International Conference on Future Nuclear Systems: Global 99, Jackson Hole, Wyoming, USA, 1999.
[3] J.D. Sullivan, P.G. Boczar, D.S. Cox, P.J. Fehrenbach, M.S. Yang, J.S. Lee, in: Proceedings of the International Conference on Future Nuclear Systems: Global 99, Jackson Hole, Wyoming, USA, 1999.
[4] I.H. Jung, K.C. Song, K.H. Kang, B.O. Yoo, Y.H. Jung, M.S. Yang, J. Metal. Mater. 5 (2001) 513.
[5] D.R. O'Boyle, F.L. Brown, J.E. Sanecki, J. Nucl. Mater. 29 (1968) 33.
[6] T. Muromura, T. Adachi, H. Takeishi, Z. Yoshida, T. Yamamoto, K. Ueno, J. Nucl. Mater. 151 (1988) 318.
[7] M.S. Yang, J.J. Park, H.S. Park, I.H. Jung, in: 11th Pacific Basin Nuclear Conference, Pembroke, Canada, 1998.
[8] H. Kleykamp, J. Nucl. Mater. 167 (1989) 49.
[9] M. Yamawaki, Y. Nagai, T. Kogai, M. Kanno, Thermodynamics of Nuclear Materials, vol. 1, IAEA, Vienna, 1980, p. 249.
[10] I. Johnson, C.E. Johnson, C.E. Crouthamel, C.A. Seils, J. Nucl. Mater. 48 (1973) 21.
[11] H. Kleykamp, J.O. Paschoal, R. Pejsa, F. Thommler, J. Nucl. Mater. 130 (1985) 426.